

First day-time seeing observations at the Observatory of University of Zanjan in Iran

Pardis Ahmadi · Neda Dadashi · Hossein Safari · Ahmad Darudi

Department of physics, P.O.Box 45371-38791, University of Zanjan, Zanjan, Iran;

Optical observatory of the university of Zanjan, University of Zanjan, Zanjan, Iran;

email: dadashi@znu.ac.ir

Abstract.

Recognition of the appropriate locations for ground-based observations of the Sun with high angular resolution depends on the factors such as seeing, meteorological and astronomical parameters. Seeing is one of the most effective parameters that could limit the quality of the observations. Therefore, to have an accurate observation, one needs to have an accurate estimation of this parameter. Using Solar Differential Image Motion Monitor (S-DIMM) method, the day-time seeing parameter is estimated for the first time at Optical Observatory of University of Zanjan, Iran. Because of hard observational conditions, the data collected at a height of 8 meters above the ground between 3rd of July to 18th of October 2018, using an 8 Inch MEAD telescope covered with a two-hole Hartman mask and a 99.99999 % solar glass filter. The results of Fried Parameter at the Observatory of University of Zanjan show a median value of 5.3 cm, with the first, and third quartiles being equal to 8.3 to 3.6 cm, respectively. The best seeing results are obtained between 9:00 to 9:30 a.m., Iran local time. Above the 6% of the measured Fried parameters are obtained to be larger than 10 cm, which seems to be better than the seeing condition at TUBITAK National Observatory, Turkey. The obtained median value of the Fried parameter during the observation period of this study is comparable with the median Fried parameters measured at good solar observatory sites, such as, Big Bear, Haleakala, La Palma, Panguitch Lake, Sacramento Peak, and San Pedro Martir, during July-September. Continuous Day-time seeing observations are needed to make a better comprehensive comparison.

Keywords: Atmospheric Effects, Site testing, Turbulence, Seeing

1 Introduction

The atmosphere of the Earth has a refractive index of about $n = 1.00029$ in the optical wavelengths at 273 K. Local random fluctuations in the temperature of the atmosphere can cause the density fluctuations, and ultimately lead to slight local changes in the refraction index of the air. As a consequence, the position of the observed star, or its' brightness would change. In some cases, multi copies of a same star (speckles) would appear in the recorded image of the star. Since the air patches in the atmosphere move with different velocities and directions all the times, the wavefront entering the telescope gets distorted and therefore, the image degradation is always expected. This effect is known as "seeing effect" and limits the angular resolution of the telescope [1, 2].

Fried 1965 introduced the r_0 parameter to describe this effect [3]. The most common method to measure the Fried Parameter, r_0 , is called DIMM (Differential Image Motion Monitors) method [4, 5, 6]. In the DIMM method, Sarazin et al. 1990, used one telescope

covered with a Hartman mask including two circular sub-apertures. One of the sub-apertures is covered with an optical wedge to ensure having two focused star images (of the same star) on the detector screen [5]. Imaging in this way with low exposure times of the order of milliseconds allows to freeze and monitor the differential image motions of the studied object. One of the benefits of the DIMM method is that the sudden shakes of the telescope, or the telescope tracking errors will affect the both images in the same way, and consequently do not affect the image separation distance.

Beckers 2001 for the first time used S-DIMM (Solar Differential Image Motion Monitor) to measure the day-time seeing parameter at NSO (National Solar Observatory, USA) [7]. Ozisik et al. 2004 used the same method to estimate the daytime seeing at the TUBITAK National Observatory in Turkey [8]. Afterward, Schamer et al. 2010, Ikhlef et al. 2012, and Song et al. 2018 used the S-DIMM to obtain an estimate of the seeing parameter on the different sites such as the 1-m Solar Telescope (SST) on La Palma, Spain [9], MISOLFA on Calern Observatory, France [10], and Mount Wumingshan in western China (with altitudes of 4,800 m, one of the candidate sites for China's Large Solar Telescope) [11].

Observatory of University of Zanjan is located in the University of Zanjan, 5 km away to the west of the city of Zanjan with latitude, longitude, and altitudes of being 36.68° North, 48.51° East, and 1638 m from sea level. Zanjan has a cold semi-arid climate with hot and dry summers and moist and cold winters with very low precipitation. The average annual precipitation, relative humidity, temperatures, and mean sunshine hours of being 315.4 mm, 53%, and 11.73°C , and 2,750 hours, respectively based on NOAA source reports [12].

In this paper, we describe the ZNU Solar-DIMM structure and the data reduction procedure, and report the first day-time seeing observation results at the Observatory of University of Zanjan in Iran. We compare the results with those of the best solar observatory sites of the world.

2 Theoretical Background

Andrey Kolmogorov 1941, provided a statistical model for describing the atmospheric turbulence [13]. In this model, the variations of the refractive index cause fluctuations of the incident light phase, which, lead to wave-front distortions. Kolmogorov considered three main turbulent length scales for a turbulent environment, namely the outer scale of turbulence L_0 , inner scale of turbulence l_0 , and an inertial range between inner and outer scales. According to this model, energy is injected to the turbulent medium via large scale (L_0) eddies. The large eddies then break up into smaller ones in a self-similar cascade until the kinetic energy is transformed into heat through the smallest eddies by viscosity phenomena [14]. Using the Kolmogorov model, the phase structure function $D_\phi(r)$ obtains as following, based on the Fried parameter value [3, 15]:

$$D_\phi(r) = 6.88 \left(\frac{r}{r_0} \right)^{\frac{5}{3}} \quad (1)$$

where, r is inertial range and r_0 is Fried parameter. r_0 is reducing with increasing the turbulence in the environment.

The variance (σ^2) of the limb image separation (in square radian) is proportional to the Fried parameter r_0 , via [16]:

$$\sigma^2 = k_l \lambda^2 r_0^{-5/3} D^{-1/3} \quad (2)$$

where, k_l , λ , and D are a constant, observing peak wavelength, and the diameter of the Hartmann mask apertures, respectively. The k_l constant is given by [16]

$$k_l = 0.364 \left[1 - 0.532 \left(\frac{d}{D} \right)^{-1/3} - 0.024 \left(\frac{d}{D} \right)^{-7/3} \right] \quad (3)$$

where d is the Hartmann mask aperture separation length. After calculating the Fried parameter from the above equations, seeing parameter (ϵ_0) can be estimated from the following formula [8]:

$$\epsilon_0 = 0.98 \frac{\lambda}{r_0} \quad (4)$$

3 Instruments, Observations, and Data Reduction

In this study, imaging was done during the best possible observing times at University of Zanjan (during the 3rd July to 18th of October 2018), from 7:00 a.m. to 10:00 a.m., using an 8 inch Meade Schmidt-Cassegrain telescope with a focal length of 2000 mm, and focal rate of f/10. The aperture is covered by a solar glass filter with 10^{-5} transmittance in the visible wavelengths. The filter has an aluminium frame, which could easily be mounted over the aperture of the telescope. A Hartmann mask with two circular apertures (with diameters, and separation distance of $D = 2.4$ cm, and $d = 15$ cm, respectively) was used in front of the solar filter. A wedge prism with a deviation angle of $82''$ was located in front of the one of the Hartmann mask holes (Fig. 1). A monochrome Meade DSI (Deep Sky Imager) CCD detector was placed in the focal plate of the telescope. It has pixels with the size of 9.6×7.5 microns, sitting in an array of 510×492 pixel square. The wedge prism is used to produce two well separated image of the solar limb at the CCD detector (the same as the procedure done in stellar DIMMs.). The instrumental parameters of the used Solar-DIMM are summarized in the Table 1.

The ZNU Solar-DIMM was placed on the terrace of the Observatory building of Zanjan University. Height of the telescope from the ground (including the telescope tripod height) was approximately 8 meters. To calibrate the r_0 measurements in cm, we need to know the image scale of the Solar-DIMM. Theoretical calculations suggest an image scale of $0.88''/\text{pixel}$ for the Solar-DIMM used in this study which is in agreement with the one obtained from the data analysis ($0.89 \pm 0.01''/\text{pixel}$).

As suggested by Sarazin and Roddier 1990, the $b = \frac{b}{D}$ ratio must be greater than 2.5 [5]. The mentioned ratio in this study is taken to be 6.25 (the similar ratio which was used by Ozisik and Ak 2004 to measure the First day-time seeing at the TUBITAK National Observatory, Turkey, [8].), to make a better comparison. The exposure time of the detector is selected to be 1 ms to be able to freeze the atmospheric changes.

Solar-DIMM can measure the seeing only in one direction. We used the transverse direction (parallel to horizon, or parallel to the aperture vector of the Hartman mask) for measuring the image motion of the solar West limb. The top panel of Fig. 2 represents two well separated images of the West limb of the sun (due to the presence of a wedge prism in-front of the one of the apertures of the S-DIMM.), taken on the 5th July, 2018 at 9:00 a.m., Observatory of University of Zanjan, Iran.

The data reduction procedure consists of several steps:

- Dark current and flat field corrections (Top panel of Fig. 2).
- Applying gradient filter on each of the frames to extract the two limb positions (Middle Panel of Fig. 2).

Table 1: Instrumental parameters of the ZNU Solar-DIMM.

Telescope	
Model	Meade Schmidt-Cassegrain
Aperture	200 mm
Focal length	2000 mm
F number	f/10
Solar filter	
Model	Glass Solar Filter
Transparency	10^{-5}
Max sensitivity	5100 Å
Hartman mask	
Aperture diameter (D)	24 mm
Aperture distance (d)	150 mm
Optical wedge	
Diameter	70 mm
Deviation Angle	82 ''
CCD camera	
Model	70 mm
Exposure time	0.001 s
pixel size	9.6×7.5 microns
array size	510×492 pixels

- Selecting a fixed direction (this direction stays the same in the all next used frames) perpendicular to the limb to make two digital slits across the limbs. Making 4 more slits parallel to the first ones, but one pixel apart from each other in upward and downward directions. Two groups, each one consists of three digital slits are created in this way. Middle Panel of the Fig. 2 shows the two groups of digital slits over the two images of a same limb, in red and blue, respectively.
- Finding the accurate limb positions of the line profiles by applying weighted Gaussian fits.
- Averaging the obtained limb positions over the two groups of digital slits, separately.
- Finding the distance between the two limb positions in each frame.
- Converting the obtained distance values (from pixel units to arcsec units) using the obtained image scale ($0.89''/\text{pixel}$).
- Calculating the standard deviation (σ) and variance (σ^2) of the limb separation values every 20 s.

According to Tokovinin 2002, having the variance of the limb separations, one can calculate the Fried parameter using Equations 2 and 3 [16]. Finally, using Equation 4, the values of the seeing parameter can be calculated.

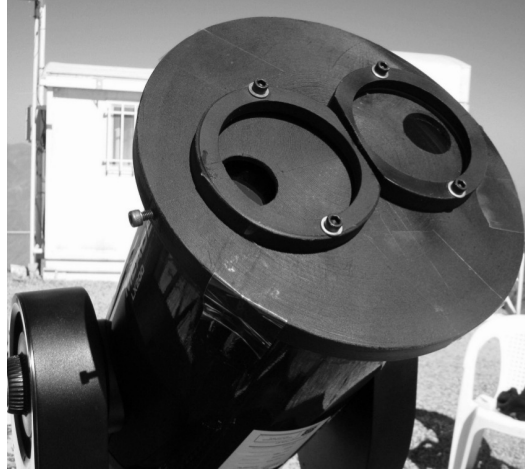


Figure 1: A Hartmann mask with two circular apertures is used in front of the solar filter at the telescope entrance. A wedge prism with a deviation angle of $82''$ is placed in front of the one of the Hartmann mask holes to make two well separated solar limb images at the focal plane.

4 First Results and Comparison

Figure 3 shows the time series of the seeing parameter from the 3rd of July to 18th of October. During July, the sky was much more clear, and the relative humidity was lower respect the other days of the observations. Therefore, a much lower seeing parameter (better seeing condition) is obtained in this month. The maximum and minimum of the seeing parameter were obtained to be $4.5''$ and $0.7''$, respectively. The mean value of the seeing parameter is obtained to be $2.6''$. Table 2 summarizes the monthly median, the first (q_1), and the third (q_3) quartiles of the measured seeing parameter for the observation times between 7:00 - 10:00 Iran local time between July to October, 2018. Seeing measurement uncertainties are calculated based on the propagation error analysis of Eqs. 2 - 4. The errors lies within ± 0.16 arcsec.

Figure 4 shows the variations of horizontal visibility and seeing parameters at 9:00 a.m. from the 3rd of July to 18th of October, 2018 at ZNU-Observatory. These two parameters show 51 % of correlation during our study period. The horizontal visibility is measured by trained human naked-eyes at Zanzan meteorological organization. This meaningful positive correlation indicates that the role of higher layer atmospheric turbulence (which is not visible by human naked-eyes on the Earth) is more prevalent than the local seeing variations for day-time seeing measurements at Observatory of university of Zanzan.

Figure 5 shows the monthly histograms of the seeing parameter. The best seeing condition is recognizable on the top-left panel of the Fig. 5, for July. The results of Fried Parameter at the Observatory of University of Zanzan show a median value of 5.3 cm, with the first, and the third quartiles being equal to 8.3 to 3.6 cm, respectively. Table 3 summarizes the median Fried Parameter at different famous solar observatory sites of the world. Above the 6% of the measured Fried parameters are obtained to be larger than 10 cm, which seems to be better than the seeing condition at TUBITAK National Observatory, Turkey. The obtained median value of the Fried parameter during the observation period of this study is comparable with the median Fried parameters measured at good solar observatory

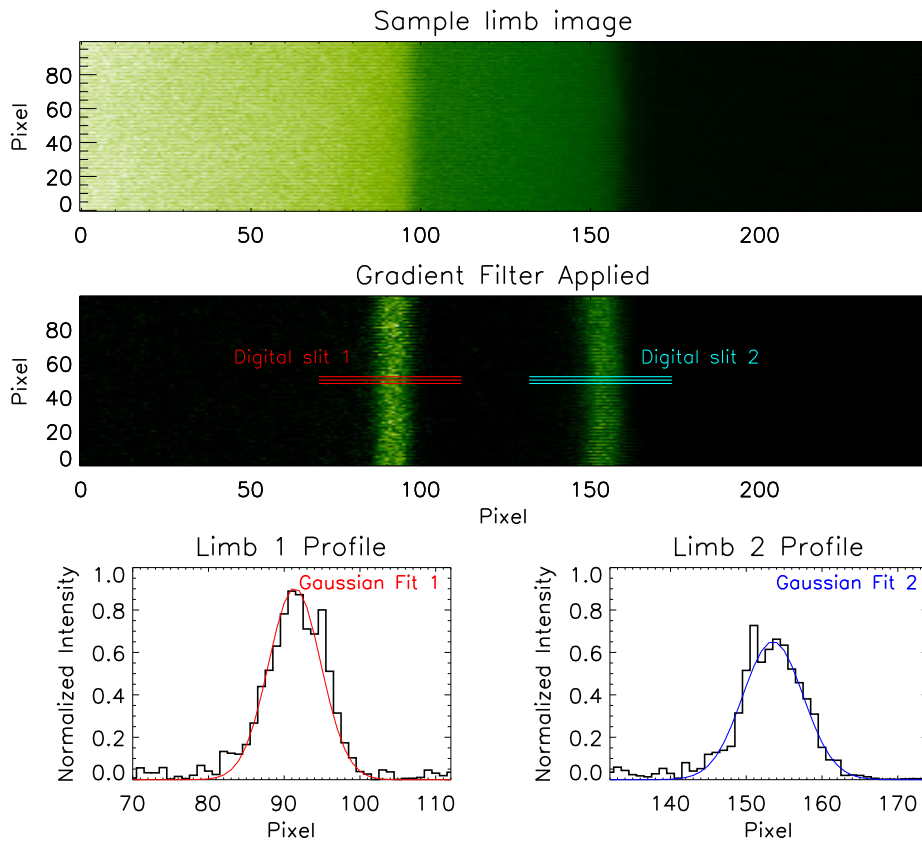


Figure 2: Top panel: A sample image of the solar West limb, taken on the 5th of July, 2018 at 9:00 a.m. using Solar-DIMM, at the Observatory of University of Zanjan, Iran. Middle panel: The same image after applying the Gradient filter. The position of the digital slits for the first and second images of the same limb are shown by red and blue lines, respectively. Bottom left panel: Normalized intensity profile of the limb 1 image. A Gaussian Profile is fitted (weighted fit with respect to the intensity errors) and overplotted on the spectrum in red color. Bottom right panel: Normalized intensity profile of the limb 2 image. A Gaussian Profile is fitted (weighted fit with respect to the intensity errors) and overplotted on the spectrum in blue color.

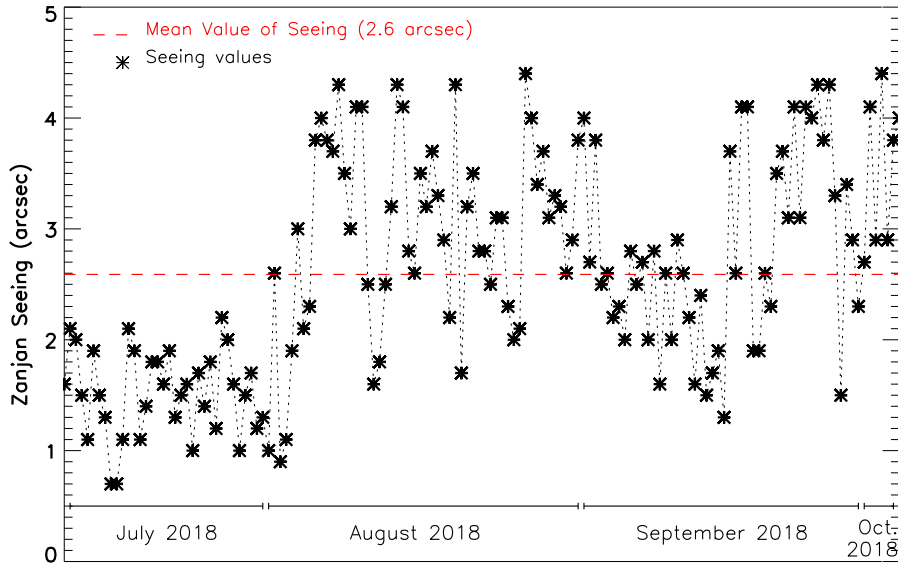


Figure 3: Time series of the seeing parameter from 3rd July to 18th October 2018 recorded at optical observatory of University of Zanzan. During July, the sky was much more clear, and the relative humidity was lower respect the other days of the observations. Therefore, a much lower seeing parameter (better seeing condition) is obtained on this month.

sites, such as, Big Bear, Haleakala, La Palma, Panguitch Lake, Sacramento Peak, and San Pedro Martir, during July-September [9, 8, 17].

Figure 6 represents the Probability Distribution Function (PDF) of the Fried parameter from the 3rd of July to 18th of October, 2018. Using the minimization of chi-square (χ^2) function, the power-law index ($-\gamma$) for a power-law function of ($P = P_0 r_0^{-\gamma}$) is obtained [18, 19]. It shows a scale-free behaviour with the power index of 2.6, which is a bit smaller than the power index value predicted and supposed by Kolmogrov ($11/3$), in his turbulence model. This deviation from the Kolmogrov turbulence model (or representing a non-Kolmogrov behaviour) could be related to the presence of the surface layer turbulence [20, 21, 22, 23, 24].

Figure 7 shows hourly Fried Parameter from the 3rd of July to 18th of October 2018, Zanzan. The red points represent the hourly average of the Fried Parameters among the all observation days. The best, and the worst seeing results are obtained between 9:00 to 9:30 a.m., and 7:15 to 7:45 a.m. Iran local time, respectively. The worst seeing condition (between 7:15 to 7:45 a.m.) might be due to the horizon dust, after the sunrise. The measured Fried parameters at this period of time has its minimum values. Therefore, the best time for solar ground-observations at the Observatoty of the University of Zanzan is reported to be between 9:00 to 9:30 a.m., Iran local time.

5 Conclusion

A Solar Differential Image Motion Monitor (S-DIMM) is used in this study to obtain the first estimations of the day-time seeing condition at the optical observatory of the University of Zanzan, Iran. The measurements are done during the period of 3rd of July to 18th of October 2018. The results, summarized in the last section, represent a rather good day-

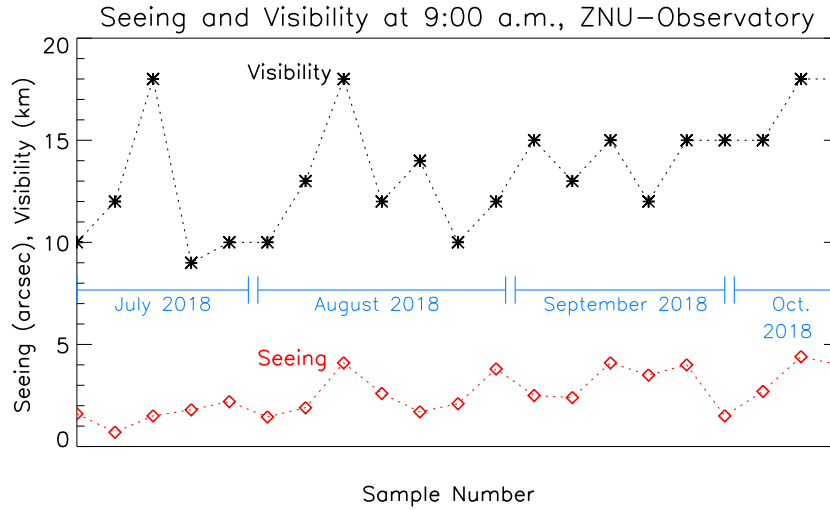


Figure 4: Variations of the horizontal visibility and seeing parameters at 9:00 a.m. from the 3rd of July to 18th of October 2018, ZNU-Observatory. These two parameters represent 51 % of correlation during our study period.

Table 2: Monthly median, first (q_1), and third (q_3) quartiles of the measured seeing parameter are shown for the observation times between 7:00 - 10:00 Iran local time between July to October 2018 (seeing measurement uncertainties lies within ± 0.16 arcsec).

Month	Day	Hours	q_1 (arcsec)	ε (arcsec)	q_3 (arcsec)
Jul.	8	15	1.09	1.37	1.67
Aug.	7	18	1.83	2.48	3.22
Sep. & Oct.	7	14	1.62	2.73	3.13
total	24	50	1.15	1.99	2.87

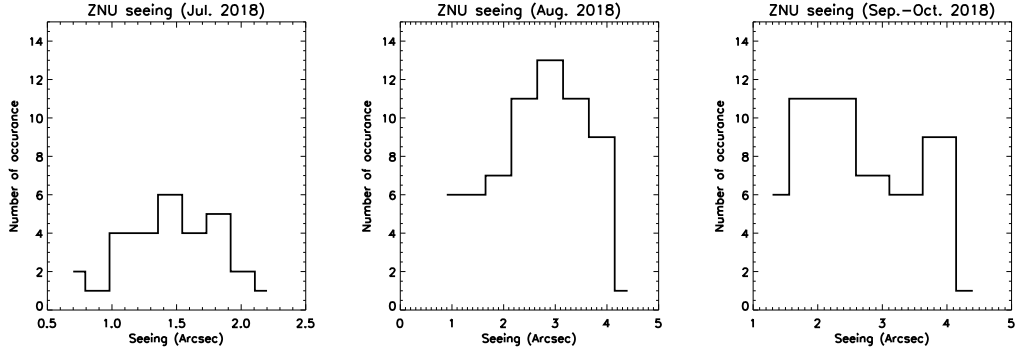


Figure 5: Histogram of the monthly seeing at ZNU-Observatory. July has the best seeing condition among the other months.

Table 3: Comparison of the median Fried parameter (cm) at famous solar observatory sites with those of obtained in this work (ZNU), during July-September [8, 17, 9]. EAM, LAM, EPM, and LPM denote early a.m., late a.m., early p.m., and late p.m., respectively.

Site (on July-September)	EAM	LAM	EPM	LPM	All day
Big Bear solar observatory, California, USA	6.34	7.13	6.50	4.93	6.45
Haleakala National Observatory (DKIST), Hawaii, USA	5.40	3.12	2.71	3.53	3.33
La Palma, Canary Island (SST), Spain	5.47	3.55	3.22	3.72	3.73
Panguitch Lake, Utah state, USA	4.15	3.63	2.92	3.53	3.59
Sacramento Peak (DST), USA	5.16	2.65	2.05	2.19	3.13
San Pedro Martir, Chile	3.91	2.66	2.19	2.42	2.73
Tubitak National observatory, Turkey	5.36	3.16	2.65	2.83	3.56
Observatory of University of Zanjan, Iran	5.30	-	-	-	-

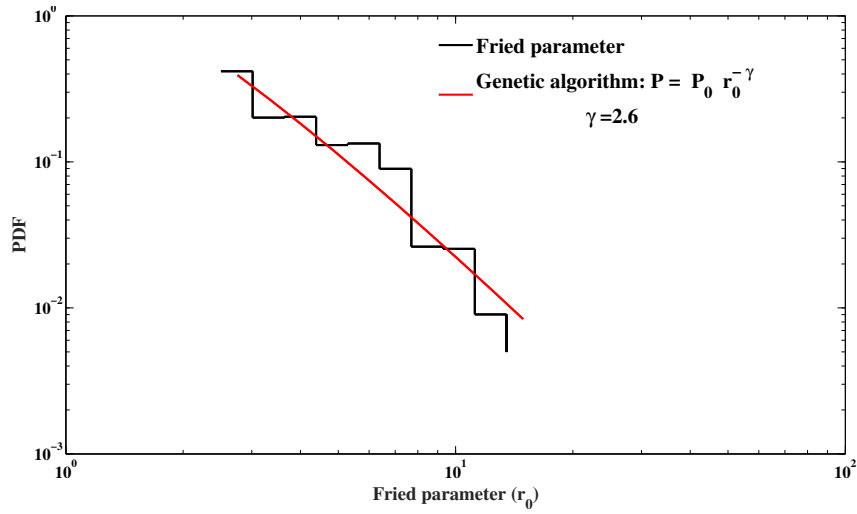


Figure 6: Probability Distribution Function (PDF) of the Fried parameter from the 3rd of July to 18th of October, 2018 shows a power-law behaviour ($P \sim r_0^{-\gamma}$) with power index of ($\gamma \simeq 2.6$), which is a bit smaller than the power index value supposed by Kolmogrov ($\gamma \simeq 11/3$), in his turbulence model. This non-Kolmogrove behaviour could be related to the surface layer turbulence [20, 21, 22, 23, 24].

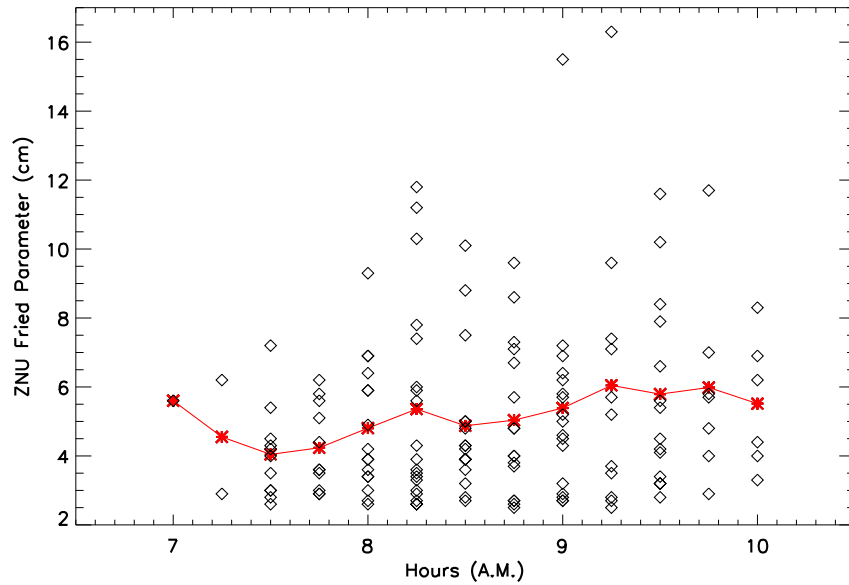


Figure 7: Hourly Fried Parameter from the 3rd of July to 18th of October 2018, Zanjan. The red points represent the hourly average of the Fried Parameters among the all observation days. The best, and worst seeing results are obtained between 9:00 to 9:30 a.m., and 7:15 to 7:45 a.m. Iran local time, respectively.

time seeing condition at the Observatory of the University of Zanjan, compared to the other famous solar observatory sites, (such as Big Bear, Haleakala, La Palma, Panguitch Lake, Sacramento Peak, TUBITAK National Observatory, and San Pedro Martir) during July-September [8]. Continuous Day-time seeing observations are needed to make a better comprehensive comparison.

Ozisik and Ak 2010 demonstrate the dependence of the wind speed to the median Fried parameter [8]. Unfortunately, the lack of having meteorological parameters, (such as, wind speed and direction, temperature, pressure, and humidity data) on the whole observation duration period, made it impossible to find any quantitative dependence between day-time seeing condition and meteorological parameters. However, we can qualitatively conclude that the highest Fried parameter obtained in July is positively correlated to the high clear sky and less humidity of this month.

The best day-time seeing result is obtained between 9:00 to 9:30 a.m., Iran local time which determines the best solar ground-observation time of this site.

Acknowledgment

The authors thank to Ms. Fatemeh Hasheminasab, Ms. Tayebeh Farjadnia, and Mr. Mahmoud Hasani for their great and kind help in gathering the seeing data. The Authors thank to Mr. Alireza Hasanloo from Zanjan Meteorological Organization for providing the horizontal visibility data.

References

- [1] Dullemond, K. 2010, Lecture notes in Observational Astronomy, Chapter 4, MKEP5, University of Heidelberg, 18-25 May.
- [2] Roddier, F. 1981, *Prog. Opt.*, 19, 281
- [3] Fried, D. L. 1965, *J. Opt. Soc. Am.*, 55, 1427
- [4] Stock, J., & Keller, G. 1961, *Telescopes. Stars and Stellar Systems.*, 138
- [5] Sarazin, M., & Roddier, F. 1990, *A&A*, 227, 294
- [6] Vernin, J., & Munoz-Tunon, C. 1995, *PASP*, 107, 265
- [7] Beckers, J. M. 2001, *Exp. Astron.*, 12, 1
- [8] Ozisik, T., & Ak, T. 2004, *A&A*, 422, 1129
- [9] Scharmer, G. B., & van Werkhoven, T. I. M. 2010, *A&A*, 513, A25
- [10] Ikhlef, R., Corbard, T., Ibrah, A., & et. al. 2012, *Understanding Solar Activity: Advances and Challenges*, 55, 369
- [11] Song, T. F., Wen, Y. M., Liu, Y., & et. al. 2018, *Sol. Phys.*, 293, 37
- [12] Zanjan Climate Normals 1961-1990. 2012. National Oceanic and Atmospheric Administration (NOAA)
- [13] Kolmogorov, A. N. 1941, *Math. Phys. Sci.*, 9, 13

- [14] Babcock, H. W. 1963, *PASP*, 75, 1
- [15] Bally, J., Theil D., Billawalla, Y., Potter, D., Loewenstein, R. F., Mrozek, F., & Lloyd, J. P. 1996, *PASA*, 13, 22
- [16] Tokovinin, A. 2002, *PASP*, 114, 1156
- [17] Rimmele, T., & Beckers, J. M. 2003, ATST site surver Working Group, ATST project
- [18] Farhang, N., Safari, H., & Wheatland, M. 2018, *ApJ*, 859, 41F
- [19] Alipour, N., Mohammadi, F., & Safari, H. 2019, *ApJS*, 243, 20
- [20] Buser, R. G. 1971, *J. Opt. Soc. Am.*, 61, 488
- [21] Bester, M., Danchi, W. C., Degiacomi, C. G., Greenhill, L. J., & Townes, C. H. 1992, *ApJ*, 392, 357
- [22] Dayton, D., Pierson, B., Spielbusch, B., & Gonglewski, J. 1992, *Opt. lett.*, 17, 1737.
- [23] Lombardi, G., Melnick, J., Hinojosa Goñi, R. H., & et al. 2010, *Proc. SPIE*, 7733, 77334D.
- [24] Bedja, A. 2010, *MNRAS*, 409, 722.